Fisheries Research 172 (2015) 79–84

Contents lists available at ScienceDirect

Fisheries Research

journal homepage: www.elsevier.com/locate/fishres

Short communication

Bruising patterns in commercially harvested yellowtail flounder (*Limanda ferruginea*)

Jessica L. Kenney, Taufiqur Rahman, Heather Manuel, Paul D. Winger*

Fisheries and Marine Institute, Memorial University of Newfoundland, 155 Ridge Road, St. John's, NL A1C 5R3, Canada

ARTICLE INFO

Article history:
Received 8 October 2014
Received in revised form 26 May 2015
Accepted 29 June 2015
Available online 24 July 2015

Keywords:
Fillet discolouration
Bruising
Image processing
Yellowtail flounder

ABSTRACT

Fillet discolouration, commonly known as bruising, is an unintended and undesirable consequence in many commercial fishing operations. The purpose of this study was to develop a method to objectively measure and characterize the size and location of discolouration patterns that are currently observed in the fillets of commercially harvested yellowtail flounder (*Limanda ferruginea)* on the east coast of Canada. To accomplish this, an image processing program was developed to analyse fillet discolouration patterns. Total discoloured area and percent fillet coverage were measured and compared to total bruise weight and percent bruise weight attained from manual assessment. Results revealed that bruising was evident in 86.5% of the fish sampled. Of all the parameters measured, fish weight was the only parameter correlated with bruise weight. Bruise area ranged from 0 to 124.5 cm^2, with a mean of 12.1 cm^2 (s.d. = 21.4), and accounted for an average of 4.3% of fillet area. Bruises were not uniformly distributed on any of the fillet sides. Results revealed a strong tendency for bruising to occur at the anterior dorsal region of the fillet, commonly known as the "nape". Functional explanations for this finding are provided, including recommendations for future research.

1. Introduction

The choice of fishing gear and handling practice employed in a fishery can play a significant role in determining the extent of discolouration (i.e. bruising) that is observed in the fillets produced. Factors known to contribute to bruising include crowding in nets, meshing, barotrauma, handling practices, method of exsanguination, and lipid oxidation (e.g. Huss, 1995; Ruff et al., 2003; Olsen et al., 2014). Bruising is observed when physical or physiological trauma causes blood vessels to rupture and blood residue to pool in certain locations. Although this discolouration has not been shown to affect the taste of fillets (Roth et al., 2007), it is disadvantageous for a number of reasons. First, blood residue within the fillets is a potential source for lipid oxidation and hydrolysis of blood cells, leading to proteolysis of the muscles, accelerating flesh softening (spoilage) post mortem (Ando et al., 1999; Grunwald and Richards, 2006). Second, from a consumer standpoint it is visually unappealing, detracting from retail value, and thus must be trimmed away prior to packaging and distribution (Robb et al., 2003; Roth et al., 2005; Olsen et al., 2006). The trimming process leads to a decrease in fillet weight, and consequently a loss in total yield and profit.

Previous research on bruise assessment and quantification has been conducted mainly in recreational fisheries, but lately to an increasing extent in commercial fisheries. Assessment has been mostly visual, with researchers often classifying bruises in terms of none, moderate or severe (e.g. Morrissey et al., 2005). Visual assessment and grading have been used in commercial fisheries for qualitatively describing discoloured fillets of rainbow trout, haddock, Atlantic cod, and Atlantic salmon (e.g. Schill and Elle, 2000; Margeirsson et al., 2007; Roth et al., 2009; Digre et al., 2010; Rotabakk et al., 2011; Olsen et al., 2013). Visual assessment of fillet discolouration has a number of benefits including its low cost, and the fact that it requires little or no complex technology, which means it can be readily performed both in the laboratory and on a vessel at sea.

One of the drawbacks of visually assessing fillet discolouration is that it can be subjective. It is difficult to ensure that assessments are consistent both between individuals and between trials, making it difficult to compare results from one study to the next. To overcome this challenge, researchers have developed a series of advanced optical, chemical, and microbiological analyses for assessing fish muscle (e.g. Grunwald and Richards, 2006; Lefèvre et al., 2008; Johnsen et al., 2011; Rotabakk et al., 2011; Olsen et al., 2013). Spectroscopy and/or image analysis software has been used to characterize discolouration (and other defects, such as gaping and nematodes) in herring *Clupea harengus* (Hamre et al., 2003),

* Corresponding author. Fax: +1 709 778 0661.
E-mail address: Paul.Winger@mi.mun.ca (P.D. Winger).

http://dx.doi.org/10.1016/j.fishres.2015.06.026

turbot *Scophthalmus maximus* (Roth et al., 2007), Atlantic cod *Gadus morhua* (Heia et al., 2007; Sivertsen et al., 2011; Olsen et al., 2014) and various salmon species (Zydlewski et al., 2008; Erikson et al., 2010; Balaban et al., 2011). The benefits of image analysis include objectivity, as well as the ability to create a reliable baseline from which to compare later research to detect the impact of changes to processing techniques.

The purpose of this study was to develop a method to objectively measure and characterize the size and location of discolouration patterns that are currently observed in commercially harvested yellowtail flounder (*Limanda ferruginea)* on the east coast of Canada. To accomplish this, an image processing program was devised to analyse fillet discolouration patterns. Total discoloured area and percent fillet coverage were measured and compared to total bruise weight and percent bruise weight attained from manual assessment.

2. Methods and materials

2.1. Frozen fish acquisition

Yellowtail flounder were harvested by Ocean Choice International during commercial fishing operations aboard the vessel F/V Aqviq. The fish were processed (i.e. gutted and bled) according to standard processing protocols and flash frozen in 23 kg blocks. They were then transported by truck from the processing facility in Marystown, NL to the Fisheries and Marine Institute in St. John's, NL, where it remained frozen at −30 °C.

2.2. Manual assessment for bruise weight

Yellowtail flounder were removed from the freezer and thawed overnight in air (14 °C) for filleting and bruise evaluation the following day. A total of 156 individual fish were sexed, measured for total length (±1 mm) and weighed (±0.1 g). The fish were then filleted and skinned, and the fillets weighed. Bruises were visually identified as regions of the fillet that were more reddish in colour than the surrounding fillet. Visible bruises were then manually removed with a filleting knife and weighed. The activity was conducted on a standard work service with indoor lighting in order to replicate a typical fish processing facility. To deal with the error associated with the subjective nature of this method, the same technician assessed and trimmed each fillet in accordance with traditional processing plant standards.

2.3. Geometric characterization of the fillets

Prior to removal of the bruises from each fillet (see above), both the outside and the inside of each fillet (left and right) were photographed on a light table to facilitate bruise detection. Each image featured two fillets with very little contrast between the background and the fillets (Fig. 1). The input images were RGB in nature, containing red (R), green (G), and blue (B) colour channels. From an image processing point of view, this lack of contrast is not ideal as it is generally difficult to segment the object of interest from the background. In order to overcome this difficulty, the contrasts between the fillets and the background, available in the three individual colour channels (red, green and blue), were taken into account. For most of the images the blue channel exhibited the most contrast with the background. Therefore, the blue channel was chosen as the primary input for the segmentation task. Image segmentation classified the pixels of the input image into two categories (object of interest and background); i.e. whether a pixel belongs to the object class or background class. A suitable gray level threshold must be determined for the segmentation task. This threshold should categorize each pixel of the input image into two groups (background

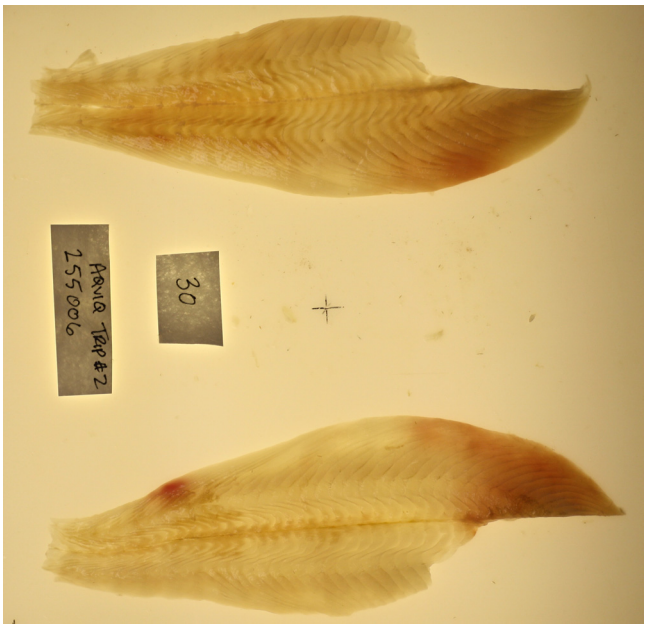

Fig. 1. Sample input RGB (red, green and blue channels) image of the outside of the left and right fillets. Bruises are defined as regions of the fillet that are darker in colour than the surrounding fillet.

or fillet) in a robust manner. Though the lighting conditions can be safely assumed to be uniform for the entire data set, a static threshold generally performs poorly and often yields unreliable results. A more robust alternative is Otsu's method, where the gray level histogram of the image is taken into account to determine an optimal threshold. Otsu's method finds the optimal threshold (Otsu, 1979) that separates the pixels into two classes in such a way that their intra-class variance is minimal. The gray level thresholds found by Otsu's method for the red, green and blue colour channels of the image as shown in Fig. 1 were 199, 166 and 98 respectively. For fillet and background segmentation, however, only the blue channel was used and the pixels were classified using the formula in Eq. (1). In Eq. (1), $I_b(i,j)$ is the gray level value of the pixel from the i-th row and j-th column in the blue channel of the input image, T_b is the threshold determined by Otsu's method from the blue channel and $B(i,j)$ is the binary value of the pixel from the i-th row and j-th column of the segmented image.

$$\mathrm{B}(i,j) = \begin{cases} 1, \text{if} I_b x < T_b \\ 0, \text{if} I_b \geq T_b \end{cases} \quad (1)$$

This step segmented the image into either blobs or background, as per standard blob analysis. Owing that the fillet was the largest object within the image, in the event smaller extraneous regions were identified, they could be safely deleted. A rigorous testing of the segmentation algorithm revealed that for most of the images, this assumption worked very well. Once the fillets were segmented, a crack code contour tracing algorithm (Wagenknecht, 2007) was employed to determine the following geometric properties of the fillets: area, perimeter, centroid, major and minor axes, vertices of the rectangle that bounds an individual fillet with minimum area. The algorithm also stored all the contour points for future reference.

2.4. Identification and localization of bruises in the fillets

In absence of any specialized lighting (e.g. UV), the image processing program depended on the chromatic properties of the bruises to identify and localize them. It was observed that the

bruised regions absorb comparatively more light. Using Eq. (2), the colour channels were inverted:

$$I_x^{\backslash} = 255 - I_x(i,j) \quad (2)$$

In Eq. (2), $I_x(i,j)$ is the gray value of any colour channel from the i-th row and j-th column, and $I^{\backslash}_x(i,j)$ is the corresponding inverted value of the corresponding pixel position. In the inverted images of the different colour channels, the bruised regions appeared to be whiter than the rest of the image. However, this distinction was not very prominent for the inverted blue channel. As a result, only the red and green channels were considered for identification and localization of the bruises. The formula in Equation 3 was then used to isolate the probable pixels that may belong to a bruised region. For the sake of clarity, it should be mentioned that $I^{\backslash}_x$ is the inverted version of the original image I_x. In addition, T_x refers to the threshold determined by Otsu's method for the x colour channel.

$$B_b(i,j) = \begin{cases} 1, \text{if} I_g^{\backslash}(i,j) > T_g, I_r^{\backslash}(i,j) > T_r \\ 0, \text{if} I_g^{\backslash}(i,j) \le T_g, I_r^{\backslash}(i,j) \le T_r \end{cases} \quad (3)$$

Once all the extraneous probable bruise regions were filtered out, a contour tracing algorithm was employed to determine the geometric properties of the bruised regions in relation to the fillet (Fig. 2). From this data, fillet areas and bruise areas were calculated, as well as the exact position of each bruise relative to the fillet's geometric centroid (the point at which the major and minor axis of the fillet intersect). Parameters of interest included the distance of the bruise from the fillet centroid as well as its angle (θ) from major axis (Fig. 2).

2.5. Analysis

The relationship between body length and weight was calculated according to the equation $W = aL^b$, where W = fish weight (g), L = fish length (mm), b (the allometric coefficient) is equal to the slope and a is equal to the intercept of the regression line of logL × logW. Condition factor was calculated as $100\,W/L^3$. Differences in fish length, fish weight, fillet weight and condition factor between males and females were compared using a one-way ANOVA. The relationship between fish length, fish weight, fillet weight and condition factor and bruise weight were measured using a correlation analysis. Values for fish length and fillet weight were log transformed to improve normality and meet the assumptions of parametric statistical analysis. A linear regression was then used to determine if fish weight, fish length and fillet weight explained variation in observed bruise weight. The differences in bruise areas between left and right fillets, and cut and skin sides of fillets were analyzed using a series of t-tests. A Rayleigh's test of uniformity was performed on bruise angles to determine whether bruises were uniformly distributed around the fillet centroid. The greater the test statistic (Z), the more closely the angles cluster around the mean vector, or the less uniform the points. Z is equal to nr^2, where n is the number of observations, and r is the length of the mean vector.

It was determined that 1 mm was equal to the length of 8.3 pixels. Fillet areas were calculated individually, and total fillet areas per fish were calculated by adding the areas of the inside of the left and right fillets. A significance level of 0.05 was used for all tests.

3. Results

3.1. Manual assessment for bruise weight

Of the 156 fish sampled, 20 were male and 136 were female. Total fish length ranged from 325.0 mm to 505.0 mm, with a mean of 399.0 mm (s.d. = 29.6). Fish weights ranged from 290.0 g to 1247.7 g, with a mean of 524.9 g (s.d. = 145.7). The fillets of the fish weighed between 90.0 g and 393.3 g, with a mean of 175.4 g (s.d. = 49.3). The total fillet weight for the entire batch was 27.36 kg. The relationship between fish length and weight was defined by the equation $W = -4.63\,L^{2.82}$ ($r^2 = 0.71$), indicating that growth in yellowtail flounder is allometric. The average condition factor of the fish (K) was 0.81, ranging from 0.37 to 1.15. See Table 1 for descriptive statistics.

Females were significantly heavier and significantly longer than males ($t_{1,155} = 3.89$, $p < 0.01$; $t_{1,155} = 2.25$, $p = 0.02$). There was no gender-related difference in condition factor ($t_{1,155} = 1.75$, $p = 0.09$) or level of bruising ($t_{1,155} = 0.92$, $p = 0.36$).

Of all 156 fish sampled, 21 (13.5%) showed no bruising, while 135 (86.5%) showed at least some bruising. Sampled fish yielded between 0.0 g and 32.1 g of bruised tissue, with a mean of 4.5 g (s.d. = 6.1). The total bruise weight for the entire sample batch was 718.1 g, a total yield loss of 2.6% by weight. Of the parameters measured, fish weight was the only one found to be correlated with bruise weight ($r^2 = 0.15$, $p = 0.03$).

3.2. Digital image analysis for bruise area

Fillet areas ranged from 176.5 cm^2 to 397.7 cm^2 with a mean of 265.4 cm^2 (s.d. = 43.4). Fillet area was well correlated with fish length, fish weight and fillet weight ($r^2 = 0.80$, $F_{1,307} = 0.90$, $p < 0.01$). Bruise area ranged from 0 cm^2 to 124.5 cm^2, with a mean of 12.1 cm^2 (s.d. = 21.4), and accounted for an average of 4.3% of fillet area. The total bruise area for the entire sample batch was 3453.3 cm^2, which was 4.26% of the entire potential yield by area. The bruised areas of the insides of the fillets were equal to the bruise areas on the outsides of fillets in both left and right fillets ($t_{1,308} = 1.05$, $p = 0.30$; $t_{1,308} = 0.61$, $p = 0.54$). For both the left and right fillet, bruise areas on the outside of the fillets were not significantly different from those on the inside ($t_{1,311} = 0.07$, $p = 0.95$; $t_{1,305} = 0.19$, $p = 0.85$). Bruise area was not correlated with fish length, fish weight, fillet weight ($n = 156$, all $p > 0.05$), but it was correlated with bruise weight ($n = 156$, $r^2 = 0.30$, $p < 0.01$).

3.3. Bruise locations

Bruises varied in their distance from the fillet centroid from 0.78 mm to 142.68 mm. They also varied in the circular distribution around the fillet centroid (see Table 2 for descriptive statistics for individual fillet information). According to the analysis, bruises were not uniformly distributed on any of the fillet sides (outside left: $Z_{1,272} = 49.21$, $p < 0.01$; inside left: $Z_{1,192} = 28.54$, $p < 0.01$; outside right: $Z_{1,374} = 39.91$, $p < 0.01$; inside right: $Z_{1,191} = 30.27$, $p < 0.01$). Angular histograms as shown in Fig. 3 revealed a strong tendency for bruising to occur at the anterior dorsal region of the fillet, commonly known as the "nape".

Table 1
Summary statistics for physical measurements taken from all fish during manual assessment.

	Minimum	Maximum	Mean	Standard deviation
Fish length (mm)	325	505	399	29.6
Fish weight (g)	290	1247.7	524.9	145.7
Fillet weight (g)	90	393.3	175.4	49.3
Fillet area (mm^2)	17650.0	39770.0	26540.0	43.4
Condition factor	0.37	1.15	.81	0.1
Bruise area (mm^2)	0.0	12450.0	1210.0	21.4
Bruise weight (g)	0.0	32.1	4.6	6.1

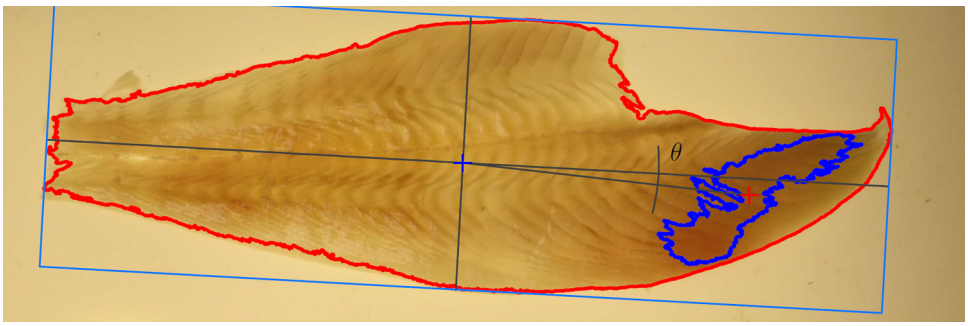

Fig. 2. Geometric characterization of a fillet and bruises. The red line represents the perimeter of the fillet, and the blue line is the perimeter of the area deemed bruised. The major (horizontal) and minor (vertical) axes of the fillet are shown. The intersection of the axes is the centroid, or geometrical centre of the fillet (blue cross). θ represents the angle of the bruise to the major axis.

Table 2
Summary statistics for bruise information collected from each side of both fillets by digital photo analysis.

	Inside left	Inside right	Outside left	Outside right
Number of bruises	193	192	273	375
Min. bruise angle (deg)	0.05	0	0.07	0.06
Max. bruise angle (deg)	359.92	359.91	360	359.91
Min. bruise distance from centroid (mm)	7.31	2.04	5.75	0.78
Max. bruise distance from centroid (mm)	142.28	127.03	142.68	137.00
Mean vector (deg)	0.44	5.23	7.79	342.99
Length of mean vector (mm)	0.38	0.39	0.43	0.33
Median (deg)	2.32	358.95	359.80	357.81
Circular variance	0.62	0.60	0.58	0.67
Circular standard deviation	79.28	77.88	75.00	85.76
Standard error of mean	7.30	7.06	5.50	6.24
Rayleigh's test (Z)	28.54	30.27	49.21	39.91
Rayleigh's test (p)	>0.01	>0.01	>0.01	>0.01

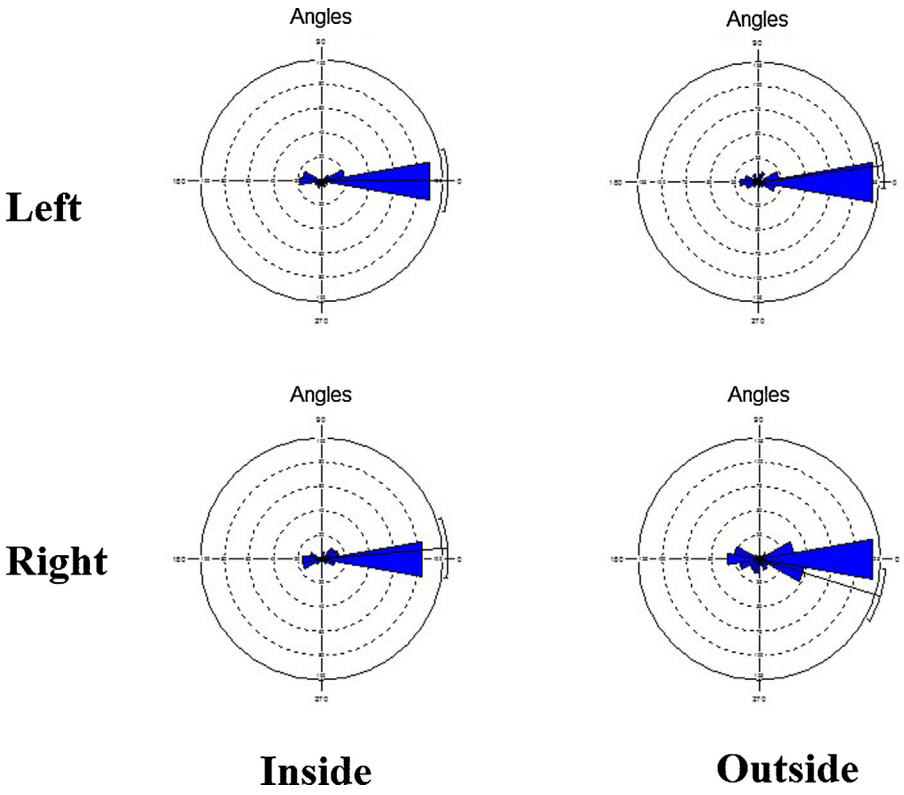

Fig. 3. Angular histograms showing a non-uniform distribution of bruise angles relative to the fillet centroid of the left and right fillets, both inside and outside. Larger cones indicate greater bruise frequencies, and the solid line radiating from the centre indicates the mean vector.

4. Discussion

4.1. Manual assessment of bruise weight versus digital image analysis of bruise area

Length and weight in yellowtail flounder was determined to be related to the equation $W = 4.63\,L^{2.82}$. The allometric coefficient, *b*, is in general agreement with previous studies conducted on flatfish, where it was found to range from 2.16 to 3.14 (Bayhan et al., 2008). Bruise weight was weakly correlated with fish weight and with no other factors, making it difficult to recommend changes to processing/harvesting that will target fish with specific characteristics such as a minimum or maximum length or weight.

Fillet area was well correlated with fish length, fish weight and fillet weight. This indicates that the image analysis program was reasonably accurate in its measurements of fillet areas, and in theory, bruise areas as well. These results build upon previous attempt to quantify fillet discolouration patterns using computer-based image processing programs (e.g. Balaban et al., 2011).

As expected, bruise area and bruise weight were found to be correlated, but not strongly. The total bruise area was 2.6% by weight, versus 4.3% by area. This difference could be due to a number of factors. First, bruises may have been removed from a thinner part of the muscle, accentuating their area rather than weight. Second, it is possible that the digital image analysis detected discolouration that would not normally be removed upon manual assessment. Yellowing or browning of the flesh is at times acceptable to leave, depending on the severity and location. Removing slight, centrally located yellowing or browning often leads to a greater profit loss than just leaving it, as a slightly yellowed fillet may still have a greater value than a fillet that has been cut into numerous pieces. Third, it is also possible that the image analysis program detected more bruising because the fillet photographs were taken on a light table, enhancing the appearance of bruising, whereas manual inspection took place on an opaque cutting board. Although not used in this study, polarized light and angular lighting techniques have been shown to improve image analysis of gaping in fillets (Balaban et al., 2011), and may have application to bruising as well.

4.2. Bruise location

Results showed that bruises in the fillets of yellowtail flounder occur mainly in the anterior region of the fillet, commonly known as the "nape", and that it was consistent for both sides of the each fillet. To our knowledge, this is the first demonstrated case where fillet discoloration (bruising) has been shown to be non-random. Previously suggested explanations for the bruising in the nape included meshing (fish being caught in the trawl during capture) and physical damage due to handling during the gutting process. By visual comparison of bruised fillets with mesh lines on the skin of the whole fish, bruising due to meshing was ruled out as a possible cause of prominent bruising in the nape of the fillets. Evaluation of gutting technique also ruled out handling during processing as a direct cause of localized bruising in the nape.

One plausible explanation of prominent bruising in the nape may be the presence of the choroid-rete, a gas-regulating organ attached to the retina of the eye of some fish (including yellowtail flounder). In conjunction with pigment cell epithelium, the choroid rete maintains O_2 pressure in the eye and supplies blood to choriocapillaries (Barnett, 1951; Wittenberg and Wittenberg, 1974). Like the rete-mirable of the swim bladder, the choroid-rete is also a counter-current exchange system composed of thousands of closely arrayed capillaries (Barnett, 1951). Lactic acid released by the retinal pigment cell layer acidifies the blood in the choriocapillaries, which causes O_2 partial pressure in the eye to increase significantly. This increase is then multiplied by the counter current exchange in the rete mirable (Wittenberg and Wittenberg, 1974; Pelster and Weber 1991; Pelster and Randall, 1998). A rapid decrease in pressure on the gas within this organ, such as the one associated with trawl retrieval to the surface, can almost certainly be expected to rupture blood vessels, leading to internal hemorrhaging, or bruising. That said, bruising was not observed in all fish, indicating other factors may be involved.

In conclusion, this study characterized the bruising patterns in commercially harvested yellowtail flounder, established a protocol for assessment of bruising, as well as a baseline level of bruising to which future levels of bruising can be compared. In order to better understand the prominence of bruising in the nape of the fillet, we recommend an anatomical investigation of the vascular system of the yellowtail flounder to determine which blood vessels are associated with the majority of bruising, and secondly, simulated decompression trials under laboratory conditions to investigate the possible effects of barotrauma.

Acknowledgements

This project was financially supported by the Natural Sciences and Engineering Research Council of Canada, Ocean Choice International, the province of Newfoundland and Labrador, and the Canadian Centre for Fisheries Innovation. Special thanks to R. Gillespie for guidance, as well as B. Gillett, M. Santos, M. Thompson and E. Posluns for technical assistance, as well as E. Durnford and T. Gill for their comments on earlier versions of the manuscript.

References

Ando, M., Nishiyabu, A., Makinodan, Y., 1999. Post mortem softening of fish muscle during chilled storage as affected by bleeding. J. Food Sci. 64, 423–428.
Balaban, M.O., Sengör, G.F.U., Soriano, M.G., Ruiz, E.G., 2011. Quantification of gaping, bruising, and blood spots in salmon fillets using image analysis. J. Food Sci. 76, E291–E297.
Barnett, C.H., 1951. The structure and function of the choroidal gland of teleostean fish. J. Anat. 85, 113–119.
Bayhan, B., Sever, T.M., Taskavak, E., 2008. Length-weight relationships of seven flatfishes (Pisces: Pleuronectiformes) from Aegean Sea. Turk. J. Fish. Aqaut Sci. 8, 377–379.
Digre, H., Hansen, U.J., Erikson, U., 2010. Effect of trawling with traditional and 'T90' trawl codends on fish size and on different quality parameters of cod *Gadus morhua* and haddock *Melanogrammus aeglefinus*. Fish. Sci. 76, 549–559.
Erikson, U., Misimi, E., Fismen, B., 2010. Bleeding of anaesthetized and exhausted Atlantic salmon: body cavity inspection and residual blood in pre-rigor and smoked fillets as determined by various analytical methods. Aquacult. Res. 41, 496–510.
Grunwald, E.W., Richards, M.P., 2006. Mechanisms of heme protein-mediated lipid oxidation using hemoglobin and myoglobin variants in raw and heated washed muscle. J. Agric. Food Chem. 54, 8271–8280.
Hamre, K., Lie, O., Sandnes, K., 2003. Development of lipid oxidation and flesh colour in frozen stored fillets of Norwegian spring-spawning herring (*Clupea harengus*). Effects of treatment with ascorbic acid. Food Chem. 82, 447–453.
Heia, K., Sivertsen, A.H., Stormo, S.K., Elvevoll, E., Wold, J.P., Nilsen, H., 2007. Detection of nematodes in cod (*Gadus morhua*) fillets by imaging spectroscopy. J. Food Sci. 72 (1), 11–15.
Huss, H.H. 1995. Quality and Quality Changes in Fresh Fish. FAO Fisheries Technical Paper No. 348. Rome FAO. 132p.
Johnsen, C.A., Hagen Ø, Adler, M., Jönsson, E., Kling, P., Bickerdike, R., Solberg, C., Björnsson, B.T., Bendiksen, E.Å., 2011. Effects of feed, feeding regime and growth rate on flesh quality, connective tissue and plasma hormones in farmed Atlantic salmon (*Salmo salar* L.). Aquaculture 318, 343–354.
Lefèvre, F., Bugeon, J., Aupérin, B., Aubin, J., 2008. Rearing oxygen level and slaughter stress effects on rainbow trout flesh quality. Aquaculture 284, 81–89.
Margeirsson, S., Jonsson, G.R., Arason, S., Thorkelsson, G., 2007. Influencing factors on yield, gaping, bruises and nematodes in cod (*Gadus morhua*) fillets. J. Food Eng. 80, 503–508.
Morrissey, M., Suski, C.D., Esseltine, K.R., Tufts, B.L., 2005. Incidence and physiological consequences of decompression in smallmouth bass and live-release angling tournaments. Trans. Am. Fish. Soc. 134, 1038–1047.
Olsen, S.H., Sorensen, N.K., Stonno, S.K., Elvevoll, E.O., 2006. Effect of slaughter methods on blood spotting and residual blood in fillets of Atlantic Salmon (*Salmo salar*). Aquaculture 258, 462–469.

Olsen, S.H., Tobiassen, T., Akse, L., Evensen, T.H., Midling Ø, K., 2013. Capture induced stress and live storage of Atlantic cod (*Gadus morhua*) caught by trawl: consequences for the flesh quality. Fish. Res. 147, 446–453.
Olsen, S.H., Joensen, S., Tobiassen, T., Heia, K., Akse, L., Nilsen, H., 2014. Quality consequences of bleeding fish after capture. Fish. Res. 153, 103–107.
Otsu, N., 1979. A threshold selection method from gray-level histograms. IEEE Trans. Syst. Man Cybern. 9 (1), 62–66.
Pelster, B., Weber, R.E., 1991. The physiology of the root effect. In: Gilles, R. (Ed.), Advances in Comparative and Environmental Physiology, Vol. 8. Springer, Berlin, pp. 51–77.
Pelster, B., Randall, D.J., 1998. The physiology of the root effect. In: Perry, S.F., Tufts, B.L. (Eds.), Fish Respiration. Academic Press, San Diego, pp. 113–139.
Robb, D.H.F., Phillips, A.J., Kestin, S.C., 2003. Evaluation methods for determining the prevalence of blood spots in smoked Atlantic Salmon and the effect of exsanguinations method on prevalence of blood spots. Aquaculture 217, 125–138.
Rotabakk, B.T., Skipnes, D., Akse, L., Birkland, S., 2011. Quality assessment of Atlantic cod (*Gadus morhua*) caught by longlining and trawling at the same time and location. Fish. Res. 112, 44–51.
Roth, B., Torrissen, O.J., Slinde, E., 2005. The effect of slaughtering procedures on blood spotting in rainbow trout (*Oncorhynchus mykiss*) and Atlantic salmon (*Salmo salar*). Aquaculture 250, 796–803.
Roth, B., Schelvis-Smit, R., Stien, L.H., Foss, A., Nortvedt, R., Imsland, A., 2007. Exsanguination of turbot and the effect on fillet quality measured mechanically, by sensory evaluation, and with computer vision. J. Food Sci. 72 (9), E525–E531.
Roth, B., Obach, A., Hunter, D., Nortvedt, R., Oyarzun, F., 2009. Factors affecting residual blood and subsequent effect on bloodspotting in smoked Atlantic salmon fillets. Aquaculture 297, 163–168.
Ruff, N., Fitzgerald, R.D., Cross, T.F., Hamre, K., Kerry, J.P., 2003. The effect of dietary vitamin E and C on market-size turbot (*Scophthalmus maximus*) fillet quality. Aquacult. Nutr. 9, 91–103.
Sivertsen, A.H., Kimiya, T., Heia, K., 2011. Automatic freshness assessment of cod (*Gadus morhua*) fillets by Vis/Nit spectroscopy. J. Food. Eng. 103, 317–323.
Schill, D.J., Elle, F.S., 2000. Healing of electroshock-induced hemorrhages in hatchery rainbow trout. North Am. J. Fish. Manage. 20, 730–736.
Wagenknecht, G., 2007. A contour tracing and coding algorithm for generating 2D contour codes from 3D classified objects. Pattern Recogn. 40, 1294–1306.
Wittenberg, J.B., Wittenberg, B.A., 1974. The choroid rete mirabile of the fish eye, I. Oxygen secretion and structure: comparison with the swim bladder rete mirabile. Biol. Bull. 146, 116–136.
Zydlewski, G.B., Gale, W., Holmes, J., 2008. Use of electroshock for euthanizing and immobilizing adult spring Chinook salmon in a hatchery. North Am. J. Aquacult. 70, 415–424.